Journal of Environmental Management 391 (2025) 126466

Contents lists available at ScienceDirect

Journal of Environmental Management

journal homepage: www.elsevier.com/locate/jenvman

Research article

Chasing net zero: An exploratory space-time analysis of European regions' industrial carbon emissions

Chiara Vagnini *, Leticia Canal Vieira, Mariolina Longo, Matteo Mura

Department of Management – University of Bologna, Via Terracini 28, 40131, Bologna, Italy

ARTICLE INFO

Keywords:
Carbon emissions
EU regions
Spatiotemporal analysis
Spatial autocorrelation method
ESTDA

ABSTRACT

Achieving a net-zero target within the European Union remains a remarkable challenge. Existing literature has predominantly examined carbon emissions at the national level, overlooking sub-national variations crucial for effective mitigation strategies. Moreover, prior studies lack a comprehensive exploration of spatiotemporal interdependencies influencing emissions dynamics within regions. We address these gaps by employing an exploratory space-time data analysis (ESTDA) to a novel panel dataset spanning 13 years and comprising carbon emissions from 238 NUTS-2 regions across 27 EU countries. The results indicate a 33.6 % decline in carbon emissions, likely driven by energy efficiency improvements and renewable energy deployment driven by European policies. However, these measures may have reached their decarbonization limit, as regional disparities in industrial emissions are narrowing and stable emission patterns persist. The study findings also indicate polarized regional clusters, often spanning multiple Member States, which follow similar decarbonization trajectories. This study applies an advanced methodological framework to a novel dataset on industrial carbon emissions across EU regions, enabling the analysis of spatial and temporal interdependencies that shape decarbonization patterns. In terms of policy implications, the findings underscore the limitations of one-size-fits-all climate strategies and emphasize the need for targeted, region-specific interventions to effectively accelerate the transition toward climate neutrality.

1. Introduction

In recent decades, the rapid increase in atmospheric greenhouse gas (GHG) concentration has driven global warming and climate change, posing a significant threat to natural ecosystems and societies worldwide. According to the latest Intergovernmental Panel on Climate Change report (IPCC, 2023), global temperature surge has occurred at an unprecedented rate over the past 2000 years. Without deep and sustained reductions in GHG emissions, global temperatures are projected to rise further, heightening the risks of natural resource depletion, biodiversity loss, heatwaves, sea-level rise, and air pollution, thereby precipitating social and humanitarian crises.

To avoid the most severe impacts of climate change, all sectors of the global economy must drastically reduce their GHG emissions, with particular urgency in the industrial sector, which has contributed 33 % of global anthropogenic emissions alone in 20,214 (Rissman et al., 2020). Governments worldwide increasingly recognize this urgency and are setting net-zero targets to balance the remaining GHG emitted into the atmosphere after implementing mitigation strategies with equivalent carbon removal (Sun et al., 2021). To keep global warming below 2 °C, emissions must reach net zero in the second half of this century and become net negative thereafter (Le Quéré et al., 2018); if the goal is to stay within 1.5 °C, net zero must be achieved around 2050 (IPCC, 2018).

Deep decarbonization requires a combination of robust innovation policy, infrastructure investments, and the deployment of advanced technologies, such as carbon capture, utilization (CCU) and storage (CCS), and hydrogen technologies (Bataille et al., 2021). The European Union (EU), as one of the largest GHG emitters (Crippa et al., 2022), has committed to achieve a 2.7 % annual reduction in emissions from 2020 to 2030 and reach net zero by 2050 (European Commission, 2019). In chasing this goal, it has taken several concrete actions: it launched the world's first international emissions trading system, implemented policy instruments to incentivize the adoption of energy-efficient technologies and practices, and directed significant investments to the European Green Deal (Vieira et al., 2022). These efforts are beginning to show results, as emissions have decreased by 5 % recently while sustaining a

* Corresponding author.
E-mail addresses: chiara.vagnini2@unibo.it (C. Vagnini), leticia.canalvieira@unibo.it (L. Canal Vieira), mariolina.longo@unibo.it (M. Longo), matteo.mura@unibo.it (M. Mura).

https://doi.org/10.1016/j.jenvman.2025.126466
Received 11 February 2025; Received in revised form 31 May 2025; Accepted 1 July 2025
Available online 8 July 2025

downward trend (Crippa et al., 2022).

Nevertheless, the pathway to net zero is not purely a technological and a political one, it is also geographical and systemic in nature (Bataille et al., 2021). To support effective action, it is necessary to deepen the understanding of the spatial context and interdependencies of the areas where emissions originate (Liu et al., 2023). Extensive research has advanced this understanding by employing spatiotemporal approaches to analyze carbon dioxide (CO_2) emissions occurrence, a major contributor to global warming (e.g., Diakoulaki and Mandaraka, 2007; Stuhlmacher et al., 2019; Grodzicki and Jankiewicz, 2022; Sporkmann et al., 2023; Fazio et al., 2024). Spatiotemporal approaches offer valuable insights into emissions' spatial distribution and temporal dynamics, thereby contributing to a detailed analysis of their evolution and impacts. Various analytical tools, such as inequality indices, trend analysis, social network analysis, and convergence methods, are commonly used to identify regional differences and spatial clusters (Liu et al., 2023). For example, Diakoulaki and Mandaraka (2007) utilized decomposition analysis to examine energy-related CO_2 emissions in 14 EU countries from 1990 to 2003, assessing their progress in decoupling emissions from industrial growth. Results indicate that while some countries have successfully reduced emissions and decoupled them from economic growth, others, such as Spain, have not effectively addressed rising emissions. Stuhlmacher et al. (2019) conducted a systematic spatio-economic assessment of the EU Emissions Trading Scheme (ETS), analyzing the spatial pattern of emissions changes from individual plants across the EU and how this pattern evolves during the scheme's first two phases. Spatial and temporal analysis revealed clustering of emissions changes at both EU and country levels, peaking at the beginning of the second phase but declining as the EU ETS matured. Specific industries such as iron and steel, coke ovens, and refining exhibit greater clustering and volatility than others.

However, the study of spatiotemporal patterns and disparities in carbon emissions across the EU has been predominantly conducted at the national level, with subnational and regional dynamics remaining relatively underexplored. Using countries as the scale of analysis may prevent accurately capturing the spatial distribution of carbon emissions across the EU due to the considerable heterogeneity of emissions observed at sub-national levels. Recent empirical research has emphasized the importance of investigating CO_2 emissions pathways at a more fine-grained geographical scale, such as the regional level, to fully grasp their inherent complexities (Mura et al., 2021). This shift is driven by the recognition that emissions patterns display significant variations within EU countries, a complexity often obscured by aggregated national-level data (Mura et al., 2021, 2023). Moreover, within EU countries, regions significantly diverge not only in terms of environmental impact but also in economic development, productive structure, resource endowments, environmental regulations, innovation dynamics, employment patterns, educational levels, and institutional quality (Rios, 2017; Peiró-Palomino et al., 2020; Barbero et al., 2021; Santoalha et al., 2021; Mura et al., 2023). Leveraging regional data allows us to account for the influence of regional idiosyncratic features. By considering local factors and challenges, this approach aids in shaping more targeted policies and breaking down mitigation targets into subnational units (Liu et al., 2022, 2023).

An additional gap in spatiotemporal studies is that prior research has mainly focused on cross-sectional characterization, overlooking interconnections and correlations of spatiotemporal elements (Liu et al., 2023). The physical proximity of locations likely plays a crucial role in CO_2 emissions, as spatial spillovers can occur (You and Lv, 2018; Baudino, 2020; Vagnini et al., 2025). Within the EU, socio-economic integration occurs through inter-regional trade, capital flows, migratory movements, and technology and knowledge transfer processes (Rios, 2017; Peiró-Palomino et al., 2020). Therefore, geographical location and spatial connectivity are likely to play a pivotal role in decarbonization. This regional integration also influences the transfer of cleaner technologies, diverse regulation settings that facilitate transboundary pollution flows, or the emulation of development models, all of which can impact on carbon emissions (Rios and Gianmoena, 2018).

This study aims to fill the identified gaps by examining how carbon emissions evolve and interconnect at the regional level across the EU. To achieve the proposed aim, we applied an exploratory space-time data analysis (ESTDA) to a novel panel dataset covering 13 years (from 2008 to 2020) of carbon emissions from carbon-intensive industrial sectors in 238 NUTS-2 regions across 27 EU countries. From a temporal perspective, the findings offer insights into the evolution of carbon emissions over time, revealing common trends such as polarization and decreasing variability. From a spatial perspective, the results reveal significant regional disparities, shedding light on the dynamics within and between macro-regional groups and their respective contributions to overall inequality. Finally, by combining the spatial and temporal dimensions, the study identifies patterns of interdependence and agglomeration in carbon emissions. It detects positive spatial correlations, geographic clusters of emissions, and their shifts over time.

The novelty of this study lies in three main contributions. First, it adopts a comprehensive and original dataset on industrial carbon emissions overtime at the EU regional level. Second, it introduces a methodological advancement over conventional statistical and traditional spatial analysis techniques by integrating global and local spatial autocorrelation analyses with a space-time transition matrix, enabling a more robust examination of carbon emissions' temporal evolution and spatial configuration (Zhang et al., 2022). Third, by revealing the spatiotemporal evolution, trends in regional disparities, polarized characteristics, and patterns of spatial aggregation of carbon emissions in EU regions, this study provides a scientific basis for regional climate governance, highlighting the limitations of a "one-size-fits-all" approach to environmental policy and emphasizing the need for targeted, region-specific interventions to accelerate the transition toward climate neutrality effectively (Baudino, 2020; Liu et al., 2023; Lian et al., 2024; Shon et al., 2024).The paper is structured as follows. Section 2 describes the research framework, detailing the data and methods employed in the analysis. Section 3 presents the results and subsequent discussion. Section 4 offers a summary of the findings along with some policy recommendations.

2. Data and methods

2.1. Research framework

Our empirical research framework is depicted in Fig. 1. We first constructed an original balanced panel dataset representing carbon emissions at the EU regional level across multiple years that comprised carbon emissions in million tons, per-capita carbon emissions, and carbon emissions per unit of industrial Gross Value Added (GVA). Subsequently, we conducted a comprehensive ESTDA with regional-level data, considering time-series variation, regional differences, spatial distribution, and agglomeration of the analyzed variables. To achieve this, we employed Kernel density estimation, Theil index decomposition, spatial distribution analysis, global and local spatial autocorrelation methods (Moran's I statistic and LISA), and space-time transition matrix. The primary purpose of the Kernel density estimation is to observe the overall data distribution of the analyzed variables over time. The Theil index decomposition gives further insights into possible disparities among regions in the level of carbon emissions, while the spatial distribution analysis provides a geographic representation of the spatial evolution of emissions levels. Moran's I statistic and LISA identify the presence of spatial dependence between carbon emissions of neighborhood regions and their spatiotemporal agglomeration, respectively. The space-time transition matrix aims to track how regions and their neighboring areas transition between different spatial emissions clusters over time.

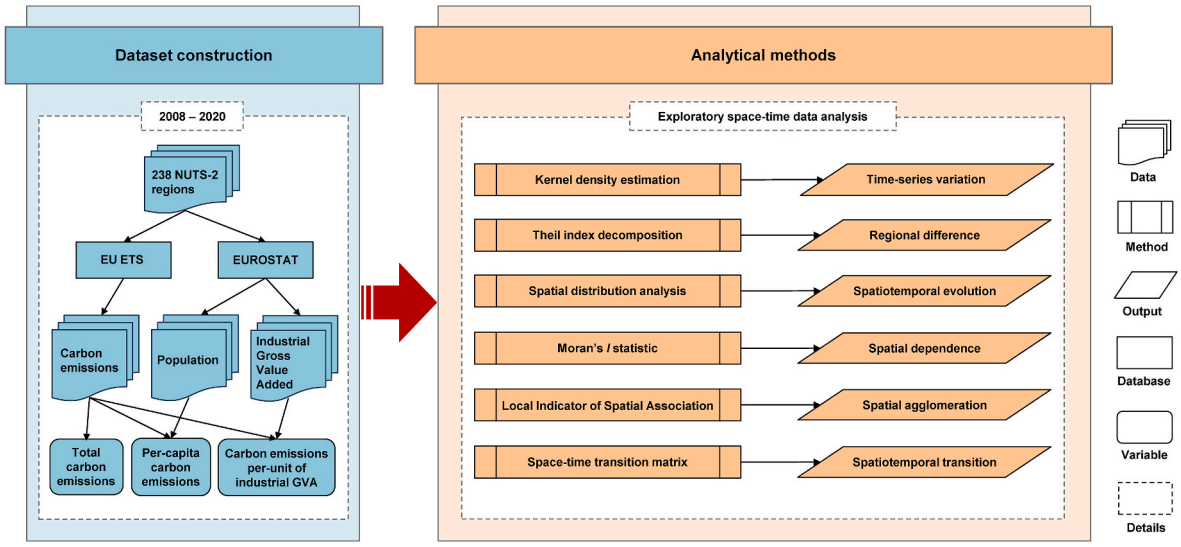

Fig. 1. Research framework (Adapted from Liu et al., 2023).

2.2. Data

Our empirical analysis utilized an original balanced panel dataset of 3094 observations. The dataset contains data on 238 regions belonging to 27 EU countries and comprises the period from 2008 to 2020. We retrieved the list of EU regions at the NUTS-2 level and used the 2016 NUTS classification by EUROSTAT. The list of regions included in the analysis is reported in Table A.1 in Appendix A.

Emissions data were sourced from the EU ETS database at the installation level[1] and then aggregated at the NUTS-2 level. Population and industrial GVA data were obtained from EUROSTAT, already available at the NUT-2 level. Table 1 contains summary statistics for the year 2020 (for a more comprehensive overview of the variables' descriptive statistics, refer to Table A.2 in Appendix A).

2.2.1. Dataset construction

EUROSTAT reports EU data on demography, economy, science and technology, and education. Data are reported at different units of analysis as EUROSTAT divides EU member states into territorial sub-units to produce regional statistics and target political interventions at a regional level (EUROSTAT, 2015). These territorial units are drawn by the Nomenclature of Territorial Units for Statistics (NUTS) classification and have been allocated a specific code and name. The NUTS classification comprises four hierarchical levels: each Member State (NUTS 0) is divided into NUTS-1 regions (i.e., major socio-economic regions), which in turn are subdivided into NUTS-2 regions (i.e., basic regions for the application of regional policies), and then divided further into NUTS-3 regions (i.e., small regions representing municipalities or counties).

We retrieved EU regions at the NUTS-2 level and used the 2016 NUTS classification, which shows 283 NUTS-2 regions in the EU. This choice was driven by the fact that the 2016 classification was the most recent one when we constructed the dataset. For reasons of missing data, we excluded all the United Kingdom (UK) regions, the Greek region *Ιόνια Νησιά*, and the Finnish region *Åland* from our sample. The UK has left the EU, and its socioeconomic data can no longer be retrieved from the EUROSTAT database or in a NUTS format. There is also no data on CO_2-eq emissions for the Greek and Finnish regions.

Table 1
Variables description and summary statistics (year 2020).

Variable	Description	Mean	SD	Min	Max
Carbon emissions	Carbon dioxide equivalent emissions (million tons) from electricity and heat generation, and energy-intensive industry sectors (oil refineries, steel works, and production of iron, aluminium, metals, cement, lime, glass, ceramics, pulp, paper, cardboard, acids and bulk organic chemicals).	5.1274	6.9479	0.0018	54.0166
Per-capita carbon emissions	The ratio of carbon dioxide equivalent emissions to the number of population at the end of the calendar year (ton/person).	3.1231	3.9993	0.0053	28.7451
Carbon emissions per unit of industrial GVA	The ratio of carbon dioxide equivalent emissions to the value-added from the NACE revision 2 sectors B-E (ton/ten thousand euros)[a].	8.7695	11.5869	0.0473	91.6536

[a] EUROSTAT provides a sectoral breakdown of economic indicators homogenized to NACE revision 2 classifications. Industrial GVA comprised GVA for the NACE rev2 Industrial (B-E) sector.

Since the NUTS classification changed during our data collection period, we ensured that the regional data was homogeneous to the 2016 NUTS classification. EU regions were reclassified in 2006, 2010, 2013,

[1] Established in 2005, EU ETS is the world's first international emissions trading system. It remains the biggest one to date, covering 11 high-energy intensity sectors and about 45 % of the total EU emissions. https://ec.europa.eu/clima/policies/ets_en.

2016, and most recently, in 2021.[2] In cases where missing values were present, we looked for whether this region had undergone reclassifications over the years (e.g., changes in the name or label or boundaries – split or merged). This process allowed us to keep most of the original observations and make the dataset as balanced and homogeneous as possible. The remaining missing values were imputed using the Multivariate Imputation by Chained Equations (MICE) algorithm[3]. To eliminate heteroskedasticity, all variables were treated logarithmically.

2.3. Methods

2.3.1. Kernel density estimation

Kernel density estimation is a nonparametric method widely employed for estimating unknown distributions of regional features due to its flexible functional form and smooth continuity (Yang et al., 2023; Xiaomin and Chuanglin, 2023; Liu et al., 2023). This approach captures the distribution shape of a random variable through a continuous probability density curve, providing insights into dynamic evolution and characteristics without requiring a predetermined function form. The formula for the kernel density estimate at any point x, derived from sample data $(x_1, x_2, \ldots, x_n)$ from the continuous distribution $f(x)$, is as follows (Rosenblatt, 1956):

$$f(x) = \frac{1}{nh}\sum_{i=1}^{n} K\left(\frac{x_i - \overline{x}}{h}\right) \tag{1}$$

$$K(x) = \frac{1}{\sqrt{2\pi}} exp\left(-\frac{x^2}{2}\right) \tag{2}$$

where $K(x)$ is a weighted or smoothing function; n denotes the number of study units; and h signifies the bandwidth. The bandwidth, influencing the variance and smoothness of the density curve, operates inversely – larger bandwidths reduce variance but increase skewness. Determining the optimal bandwidth involves balancing variance and skewness to minimize mean squared error, a task exemplified by setting $x = 0.9SeN^{-0.2}$, where Se represents the standard deviation of the observed random variable in a Gaussian kernel distribution function.

2.3.2. Theil index decomposition

The Theil index, which was introduced by Theil (1967), serves as a significant measure for evaluating regional inequalities and has gained extensive application in analyzing differences in regional carbon emissions (Xiao et al., 2019; Zhang and Li, 2022; Liu et al., 2023). Its key advantage lies in breaking down the overall difference into within-group inequality and between-group inequality, providing a clear understanding of the direction and magnitude of each variability within the total difference. In this study, we employ the Theil index to assess the inequality within and between four distinct macro groups of regions (northeast, eastern, central, and western – refer to Fig. 2) of carbon emissions across EU regions. The formulation of the Theil Index is articulated as follows:

$$T = \sum_{j=1}^{M}\sum_{i=1}^{N}\frac{y_{ij}}{Y}\log\left(\frac{y_{ij}/Y}{x_{ij}/X}\right) \tag{3}$$

where y_{ij} is carbon emissions of i region of j group, Y is carbon emissions of all regions in all groups $\left(\sum_{j=1}^{M}\sum_{i=1}^{N} y_{ij}\right)$ or the total EU regions' carbon emissions, x_{ij}/X equals one divided by the number of all regions in all groups $\left(\sum_{j=1}^{M}\sum_{i=1}^{N} x_{ij}\right)$. From equation (3), the decomposition equation of the Theil Index can be expressed as follows (see Appendix B):

$$T = T_B + T_W \tag{4}$$

where T_B and T_W represent between- and within-group inequalities, respectively. T_B can be calculated through the following equation:

$$T_B = \sum_{j=1}^{M}\frac{Y_j}{Y}\log\left(\frac{Y_j/Y}{X_j/X}\right) \tag{5}$$

where Y_j means total carbon emissions of j group, and X_j indicates the number of regions in the j group. T_W can be measured as:

$$T_W = \sum_{j=1}^{M}\frac{Y_j}{Y}\left[\sum_{i=1}^{N}\frac{y_{ij}}{Y_j}\log\left(\frac{y_{ij}/Y_j}{x_{ij}/X_j}\right)\right] \tag{6}$$

where x_{ij}/X_j is equal to one divided by the number of regions in j group. Theil index ranges from 0 to 1, with a higher value indicating greater differences in regional carbon emissions.

2.3.3. Spatial autocorrelation method

Spatial autocorrelation reveals the intrinsic similarity of data at a given location with that of other locations (Anselin, 2001). There is a positive spatial autocorrelation when high or low values of a random variable tend to cluster in space, whereas there is negative spatial autocorrelation when geographical areas tend to be surrounded by neighbors with very dissimilar values. On the contrary, if the spatial distribution of a variable within an area is uneven and random, it is referred to as spatial heterogeneity.

Spatial autocorrelation is divided into global spatial autocorrelation and local spatial autocorrelation. The global spatial autocorrelation provides information about whether a research object tends to geographically cluster in areas that are similar to each other or it follows a random geographical distribution. The most commonly used index is the global Moran's I statistic (Moran, 1948; Cliff and Ord, 1981), which calculates the spatial correlation and heterogeneity of CO_2 emissions for region i and year t is as follows:

$$I_t = \frac{\sum_{i=1}^{N}\sum_{j=1}^{N} w_{ij}\left(x_{i,t} - \overline{x_t}\right)\left(x_{j,t} - \overline{x_t}\right)}{S^2\sum_{i=1}^{N}\sum_{j=1}^{N} w_{ij}} \quad t = 1, \ldots, T \tag{7}$$

$$S^2 = \frac{\sum_{i=1}^{N}\left(x_{i,t} - \overline{x_t}\right)^2}{n} \tag{8}$$

where S^2 is the sample variance; $x_{i,t}$ and $x_{j,t}$ are the CO_2 emissions values in region i and region j, respectively, in year t; $\overline{x_t}$ is the average CO_2 emissions for all regions in year t; w_{ij} are the elements of the spatial weights matrix W; and $\sum_i\sum_j w_{ij}$ represents the sum of all the weights.

The spatial weight matrix W is a $n \times n$ matrix, where the spatial weights w_{ij} are 1 when i and j are neighbors, and zero otherwise. In most of the cases, the binary zero-one weights are *row-standardized*, that is divided by the row sum. As a result, each row sum of the row-standardized weights equals one, and the sum of all the weights, $\sum_i\sum_j w_{ij}$, equals the number of observation n. Different spatial weighting matrices are available, and fundamental consideration is given to the choice of which matrix to apply for the spatial calculation, as different matrices may yield different results (Anselin, 1988; Anselin and Bera, 1998).

The global Moran's I index ranges between [−1, 1]; values greater

[2] Changes from NUTS 2016 to NUTS 2021 level-2 classification affected our dataset for the Croatian region *Kontinentalna Hrvatska* (HR04) only, which had been split into three regions in the 2021 version: *Panonska Hrvatska* (HR02), *Grad Zagreb* (HR05), and *Sjeverna Hrvatska* (HR06).

[3] We employed MICE using the Classification and Regression Trees (CART) method. The CART method was selected within the MICE framework because it is well-suited to handling both linear and nonlinear relationships and is robust to outliers and multicollinearity, which can be common in regional panel data.

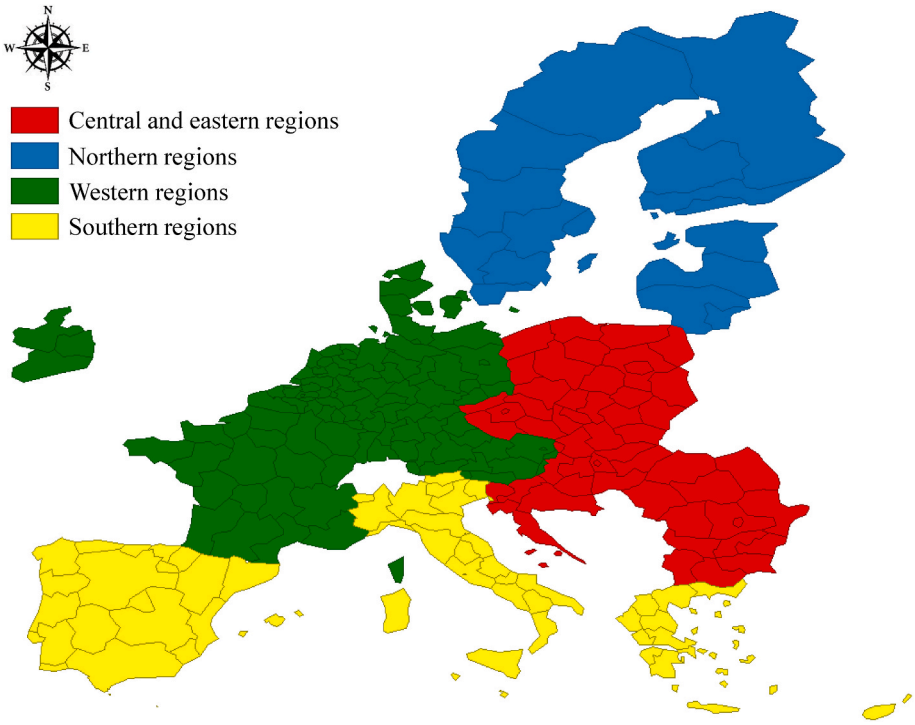

Fig. 2. Classification of the study area into four macro groups of regions.[41]

than zero mean positive spatial correlation, while lower than zero negative spatial correlation.

Global spatial autocorrelation assesses the global spatial pattern and does not indicate the location of spatial autocorrelation. Local spatial autocorrelation can be analyzed using the Moran scatterplot (Anselin, 1996), which plots the standardized spatial lag values of the variables under study (y-axis) against thier original standardized values (x-axis). The scatterplot creates four different quadrants that denote the four spatial agglomeration types between a region and its neighbors: 1) High-High (HH), a region with a high value surrounded by regions with high values, 2) High-Low (HL), a region a with high value surrounded by regions with low values, 3) Low-Low (LL), a region a with low value surrounded by regions with low values, and 4) Low-High (LW), a region a with low value surrounded by regions with high values. Quadrants HH and LL refer to positive spatial autocorrelation, whereas HL and LH indicate negative spatial autocorrelation (i.e. atypical localizations). However, the Moran scatterplot does not show the significance of the spatial clustering. To remedy this situation, Anselin (1995) introduces a Local Indicator of Spatial Association (LISA), which has two important characteristics: first, the LISA provides a statistic for each observation with an assessment of significance; second, it establishes a proportional relationship between the sum of the local statistics and a corresponding global statistic. The method of calculating the local version of Moran's *I* statistic for CO_2 emissions of each region *i* and year *t* is defined as:

$$I_{i,t} = \frac{(x_{i,t} - \overline{x_t})}{S^2} \sum_{i=1}^{N} w_{ij}(x_{j,t} - \overline{x_t}) \quad t = 1, \ldots, T \tag{9}$$

where $x_{i,t}$ are CO_2 emissions values in region *i* in year *t*; $\overline{x_t}$ is the average CO_2 emissions for all regions in year *t*; w_{ij} are the elements of the spatial weight matrix *W*.

The combination of Moran scatterplot statistics with the significance of LISA generates a visual map in which regions with significant Moran's *I* statistic are coloured according to the quadrant they belong (Anselin and Bao, 1997).

The spatial weight matrix used in this study is the 10 nearest neighbors (10nn) calculated from the inverse squared distance between region centroids. Compared to the US and China, the sample of European regions is less compact, with an average of 5–6 contiguous neighbors per region. Our choice of 10nn yields a ring around each region of approximately the first and second-order contiguous regions and connects the UK and some islands such as Sicilia, Sardegna, and Baleares to continental Europe. The inverse squared distance feature is chosen to avoid spurious neighboring relations, as it assumes that the local influence of a region on its neighbors decays with the growing distance. Furthermore, the matrix is normalized according to row standardization to interpret the spatial spillover effects as an average of all neighboring regions.

2.3.4. *Space-time transition*

Building on the exploration of spatial dependence through LISA, Rey (2014) introduced the concept of space-time transition by incorporating the properties of distance, orientation, and cohesion of each unit in a Moran plot into a Markov chain. Space-time transitions are categorized into four types: Type I, Type II, Type III, and Type IV.

- Type I signifies a transition occurring within the region itself, with no changes in the neighborhood. Examples include $HH_t \rightarrow LH_{t+1}$, $HL_t \rightarrow LL_{t+1}$, $LH_t \rightarrow HH_{t+1}$, and $LL_t \rightarrow HL_{t+1}$.
- Type II indicates that the unit itself remains unchanged, but transitions occur in the neighborhood. This involves scenarios like $HH_t \rightarrow HL_{t+1}$, $HL_t \rightarrow HH_{t+1}$, $LH_t \rightarrow LL_{t+1}$, and $LL_t \rightarrow LH_{t+1}$.
- Type III involves transformations in both the unit itself and its neighborhood, further divided into Type III_A and Type III_B. The former represents the same orientation between the unit and the neighborhood (e.g., $HH_t \rightarrow LL_{t+1}$ and $LL_t \rightarrow HH_{t+1}$), while the latter indicates opposite orientations (e.g., $HL_t \rightarrow LH_{t+1}$ and $LH_t \rightarrow HL_{t+1}$).
- Type IV indicates no transitions either in the unit itself or in the neighborhood, all of which align with the main diagonal of the transition matrix.

Spatial stability, denoted as S_t, is defined as:

$$S_t = \frac{F_{0,t}}{m} \tag{10}$$

where $F_{0,t}$ denotes the number of regions with Type IV transitions in time period t, and m is the total number of regions where the transition is likely to occur. The spatial stability index S_t ranges from 0 to 1, with a larger value signifying stronger spatial stability.

3. Results

3.1. Time evolution of EU carbon emissions

The carbon emissions landscape within the EU regions showcased a continuous and rapid decline over the observed period from 2008 to 2020 (Fig. 3). These trends collectively indicate a positive shift towards lower carbon emissions, implying notable improvements in the carbon efficiency of industrial activities.

Carbon emissions in million tons initially exhibited a variable trend, beginning at 1.839 billion tons in 2008 and continuing to fluctuate over the subsequent years. The emissions declined from 1.839 to 1.633 billion tons between 2008 and 2009, likely reflecting the impact of the global financial crisis. Subsequently, emissions increased to 1.687 billion tons in 2010, signalling economic recovery and higher output from industrial activities. However, in the following years leading up to 2015, the emissions experienced a nuanced decline, reaching 1.594 billion tons. The subsequent period from 2016 to 2020 witnessed a more notable decrease, with emissions falling to 1.220 billion tons, reflecting a substantial overall rate of decline of 33.6 %.

At the same time, per-capita carbon emissions showed a consistent downward path, dropping from 4.184 tons/person in 2008 to 2.729 tons/person in 2020, resulting in an impressive overall decrease of 34.8 %. Political elements, like the commencement of the EU ETS phase 3 in 2013 and the approval of the Paris Agreement in 2015, have indicated an evident dedication to climate mitigation that could have encouraged emissions reduction.

In parallel, the aggregated carbon emissions per unit of industrial GVA followed a decreasing pattern, declining from 9.072 ton/ten thousand euros in 2008 to 5.415 ton/ten thousand euros in 2020. This noteworthy reduction indicates a significant decrease in the carbon intensity associated with economic output in the industrial sector, with an overall rate of decline of 40.3 %. This variable has experienced the most substantial decline between the variables under examination, and the intensity of emissions has been consistently decreasing throughout our study period. The incremental trend of decline present in carbon emissions per unit of industrial GVA might be a signal that companies are still focusing on productive processes that are more energy and carbon-efficient; however, no significant technological change that could create a sudden substantial drop in emissions has happened.

Fig. 4 illustrates kernel density estimates portraying the distribution of carbon emissions in million tons, per-capita carbon emissions, and carbon emissions per unit of industrial GVA across EU regions during the observed years (2008, 2014, 2020). The shape of the density curves remained relatively consistent, showcasing a stable overall trend in the skewness of carbon emissions for the three analyzed variables. However, there was a significant increase in the crest height. This indicates that a substantial portion of the data is clustered closely, possibly in regions with similar emission levels. Despite this localized concentration, the narrowing trend observed in the width of the curve implies that the overall variability of carbon emissions across regions was decreasing. Thus, an intense concentration of emissions within a certain range is followed by differences between regions' emission levels becoming less

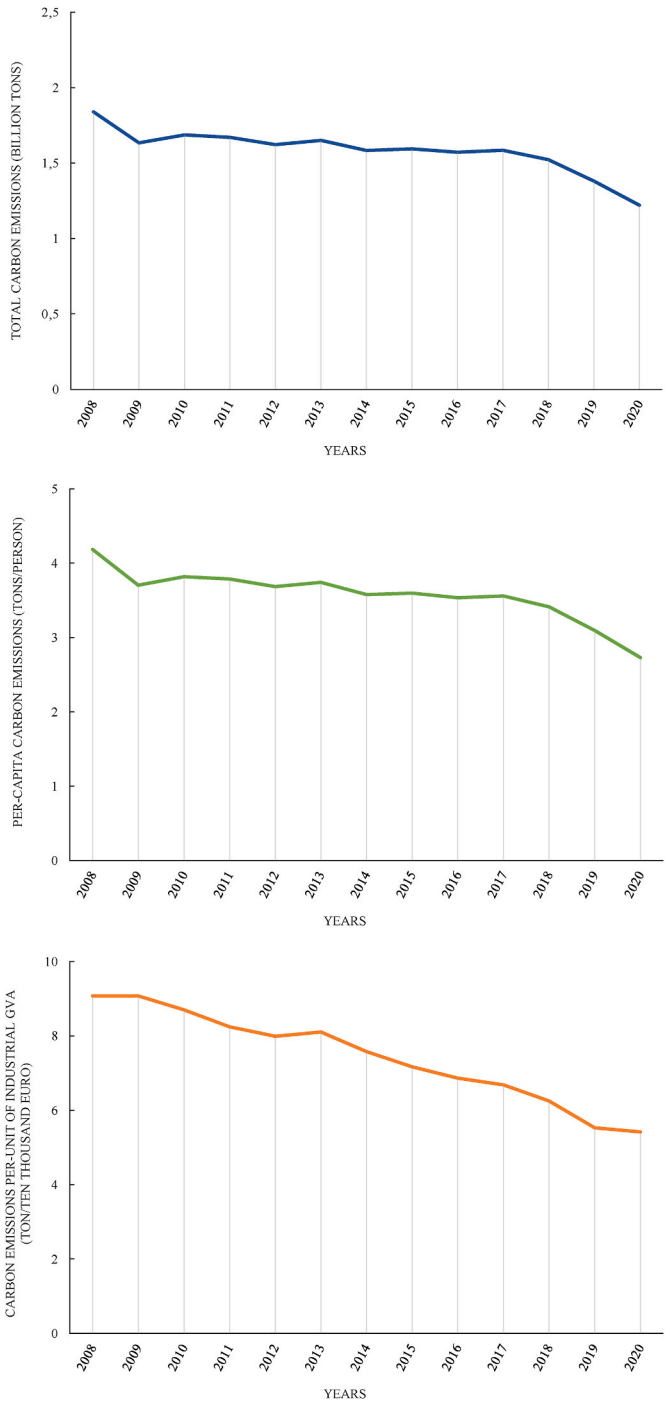

Fig. 3. Total of carbon emissions in million tons, per-capita carbon emissions, and carbon emissions per unit of industrial GVA in the EU.

pronounced. The implementation of stringent environmental regulations and incentives for renewable energy adoption in the European context are features that assist in explaining this trend. Additionally, technological developments and improvements in energy efficiency practices likely played a crucial role in reducing carbon emissions, further narrowing the gap between high and low-emission regions. The subtle leftward shift in the distribution curve is noteworthy, signifying a gradual decline in carbon emissions. Moreover, the variability in the curve's tail suggested that there is a narrowing gap between regions with high carbon emissions. In other words, it implies that disparities are decreasing among regions with higher emissions. In summary, these results confirmed the significant decline in emissions observed across

[4] European subregions classification defined by EuroVoc in the 7206 Europe: Concept Scheme: https://op.europa.eu/en/web/eu-vocabularies/concept-scheme/-/resource?uri=http://eurovoc.europa.eu/100277.

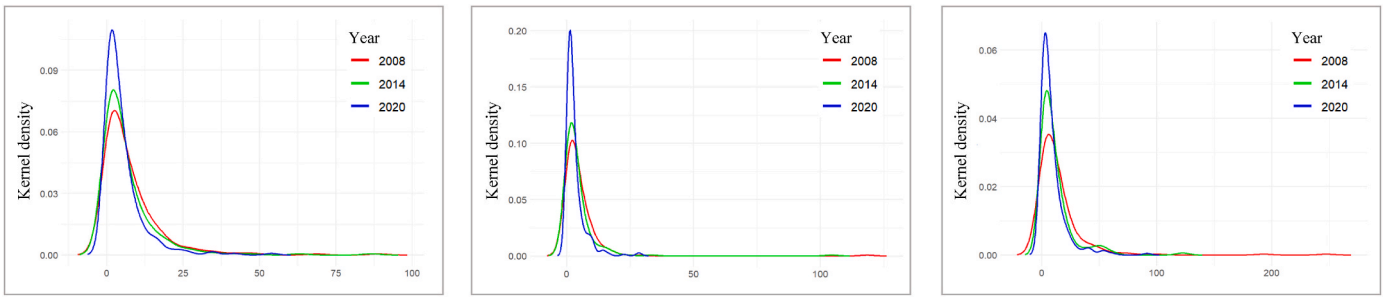

(a) Carbon emissions in million tons (b) Per-capita carbon emissions (c) Carbon emissions per unit of industrial GVA

Fig. 4. Kernel density estimation curve of regional carbon emissions in the EU.

the EU in the previous findings and revealed an increase in emissions variability across EU regions.

3.2. Regional differences of carbon emissions

As depicted in Fig. 5a_1, the regional disparities in carbon emissions in million tons across EU regions exhibited an overall decreasing trend from 2008 to 2020, with the Theil index declining from 0.26 to 0.22, marking a 14.8 % decrease. The Theil index analysis also revealed that the evolution of within-group differences closely mirrored the overall trend, primarily driven by within-group disparities during this period, accounting for an average contribution of 98.3 % (Fig. 5a_3). Furthermore, the between-group difference fluctuates but does not show a clear trend, indicating that differences between macro-defined groups in the EU have not consistently increased or decreased. However, it overall demonstrated a decreasing trend between 2008 and 2020, experiencing a notable 63.84 % reduction in the Theil index (Fig. 5a_2).

Similarly, there was a discernible decrease in regional disparities in per-capita carbon emissions, amounting to an overall reduction of 14.8 % (Fig. 5b_1). The evolution of within-group differences in this aspect broadly aligned with the overall trend, contributing, on average, 98.3 % to the overall change (Fig. 5b_3).

Additionally, regional disparities in carbon emissions per unit of industrial GVA over the study period are quite volatile but show a general downward trend, indicating a total reduction in disparities of 12.4 % (Fig. 5c_1). The between-group Theil index (Fig. 5c_2) decreases over time, which suggests that the differences between-group in terms of emissions per unit of industrial GVA are becoming less pronounced, while the within-group Theil index (Fig. 5c_3) is also volatile with a slight downward trend, indicating a reduction in disparities within groups over time.

Overall, there is a trend of decreasing regional disparities in carbon emissions, both in absolute terms (million tons) and when adjusted for population and economic output. This convergence may be driven by multiple elements, including EU-wide environmental policies, the spread of green technologies, and economic convergence among EU regions. Within-group differences have generally decreased, especially in the latter part of the timespan. This suggests that regions within the same macro geographical classification are becoming more similar regarding carbon emissions. Between-group differences, however, are

Fig. 5. Regional differences of carbon emissions in the EU during 2008–2020.

more mixed and show significant volatility, suggesting that a range of underlying factors, such as economic structure or the implementation of environmental policies, can influence broader differences between these groups.

3.3. Spatial distribution of regional carbon emissions

The spatial analysis presented in Fig. 6 highlights a pronounced heterogeneity in the distributions of carbon emissions in million tons, per-capita carbon emissions, and carbon emissions per unit of industrial GVA across EU regions. The consistent reduction trend observed across all emission categories signifies promising advancements in curbing carbon output. This decline suggests a dynamic interplay of diverse factors shaping emission patterns, aligning with sustainability goals. Furthermore, it signals adaptability and positive transformations within EU regions, indicative of a broader shift towards a more environmentally friendly economy (i.e., the decline in coal usage and the upsurge in renewable energy sources). The trend may indicate widespread adoption of cleaner technologies across various industries, reflecting a collective commitment to sustainable practices and a greener future.

Despite the overall declining trend, approximately 17 % of the regions consistently maintain higher emissions, with notable spikes (>50 %) in Région de Bruxelles (Belgium), Ανατολική Μακεδονία, Θράκη (Greece), Nyugat-Dunántúl (Hungary), and Flevoland (the

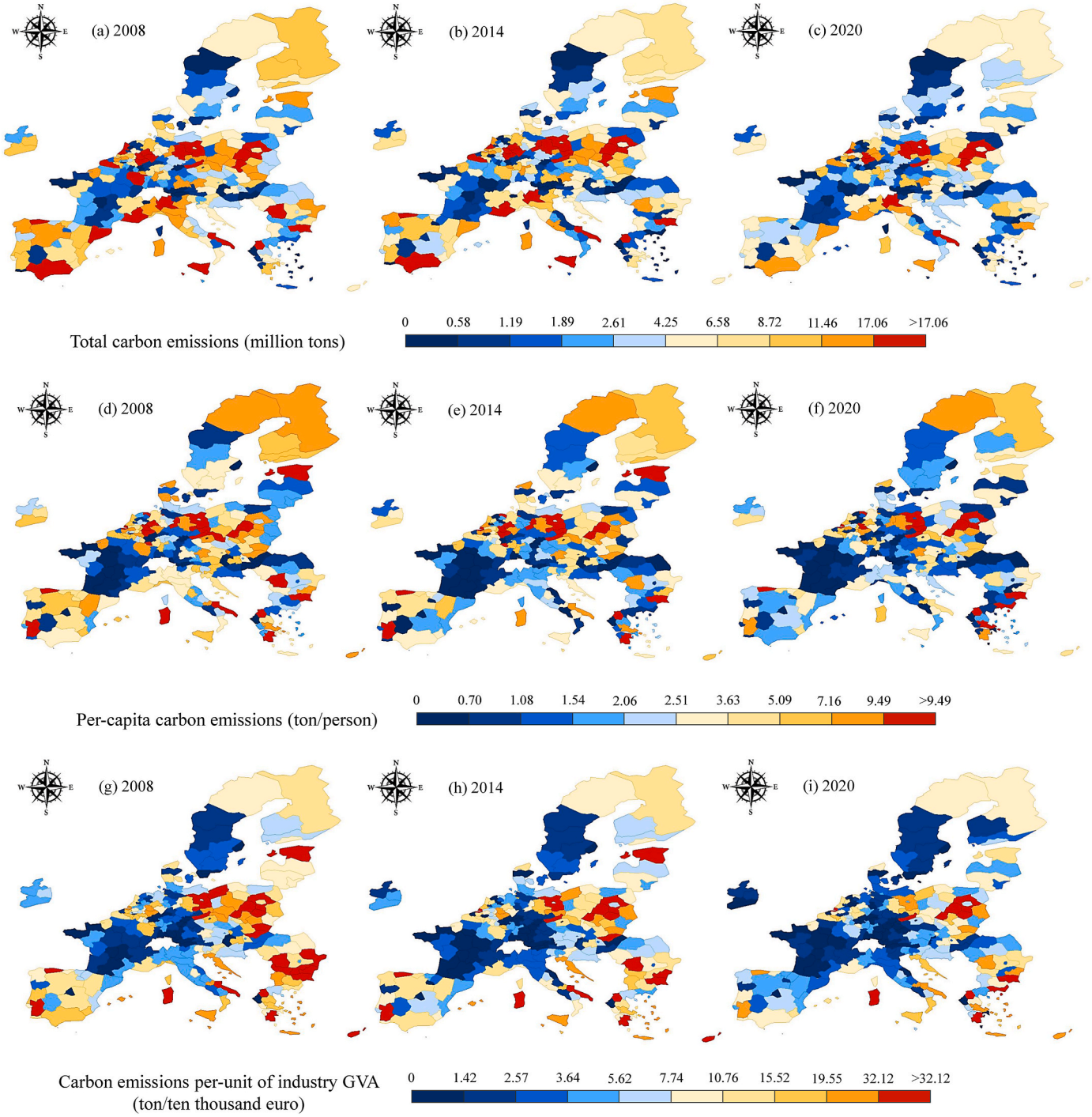

Fig. 6. Spatiotemporal evolution of regional carbon emissions in the EU.

Netherlands). This divergence could be attributed to local economic structures, heavy industry prevalence, energy production methods, or regional environmental policies.

Regarding carbon emissions in million tons, regions characterized by heightened industrial activities or larger populations consistently register elevated total emissions. Certain European regions, particularly those in Germany, the Benelux countries, Northern Italy, and some Central and Eastern European regions, stand out for their substantial emissions, driven by concentrated industrial operations. In contrast, Western and Northern regions report lower total emissions, potentially reflecting the interplay between industrialization, economic structure, and environmental policies. The disparity becomes even more apparent when scrutinizing per-capita emissions: Scandinavian regions exhibit lower per-capita emissions, attributed to their substantial investments in renewable energy and sustainable technologies. Conversely, regions with intensive industries but lower population densities, such as certain Eastern European areas, might display higher per-capita emissions. This contrast intensifies when delving into carbon emissions per unit of industrial GVA. Regions with advanced economies (higher industrial GVA) yet lower emissions per industrial GVA unit, exemplified by parts of western and northern European regions, may suggest more efficient and cleaner industrial practices. Eastern and Central regions present an increase in carbon emissions per unit of industrial GVA, emphasizing the pressing need for targeted interventions. This stark divergence emphasizes the unique paths regions in the EU are taking regarding emissions, necessitating nuanced and region-specific strategies to navigate the intricate landscape of decarbonization.

3.4. Spatial agglomeration of regional carbon emissions

Table 2 delineates the evolution of the global Moran's index across the years, indicating a noteworthy positive and significant spatial correlations in the distribution of carbon emissions across EU regions. During the specified timeframe, the Moran's index demonstrates a subtle but consistent upward trend. This suggests a developing spatial clustering trend in EU regions, indicating that regions are likely to be neighboured by areas with comparable levels of carbon emissions. Geographic proximity might facilitate inter-firm collaborations, exchange of knowledge, and labour mobility, which might result in regions following similar development pathways (Boschma and Frenken, 2006; Rios and Gianmoena, 2018).

The clustering of carbon emissions in the EU was relatively robust, with HH and LL configurations emerging as the dominant forms of local spatial autocorrelation (Fig. 7). In terms of carbon emissions in million tons, HH and LL configurations constituted a significant portion, accounting for 26.5 % and 41.2 % of all types in 2008. By 2020, these percentages changed to 28.3 % and 32.6 %, respectively, indicating an increase in HH clusters and a reduction in LL clusters. In contrast, the proportion of LH and HL increased from 26.5 % to 5.9 % in 2008 to 30.4 % and 8.7 % in 2020, respectively. Furthermore, the ratio of HH and LL patterns in per-capita emissions changed from 18.2 % to 39.4 % in 2008 to 25.3 % and 38.5 % in 2020. Simultaneously, LH and HL patterns moved from 33.3 % to 9.1 %–29.7 % and 6.6 %. In the context of carbon emissions per unit industrial GVA, HH and LL patterns evolved from 20.9 % to 59.1 % in 2008 to 25.2 % and 55.7 % in 2020. Meanwhile, LH and HL patterns shifted from 10.9 % to 9.1 % in 2008 to 13.9 % and 5.2 % in 2020. In other words, the HH cluster demonstrates an uptrend in CO_2 emissions in million tons, per-capita CO_2 emissions and CO_2 emissions per unit of industrial GVA.

Table 2
Global Moran's I statistics for carbon emissions in million tons.

Year	Moran's I	E[I]	mean	sd	z-value
2008	0.0924***	−0.0042	−0.0042	0.0253	3.8212
2009	0.0991***	−0.0042	−0.0042	0.0254	4.0687
2010	0.1062***	−0.0042	−0.0042	0.0253	4.3702
2011	0.0968***	−0.0042	−0.0042	0.0254	3.9918
2012	0.0981***	−0.0042	−0.0042	0.0252	4.0075
2013	0.1174***	−0.0042	−0.0042	0.0251	4.8310
2014	0.1175***	−0.0042	−0.0042	0.0251	4.8473
2015	0.1010***	−0.0042	−0.0042	0.0251	4.1867
2016	0.1053***	−0.0042	−0.0043	0.0250	4.3728
2017	0.0973***	−0.0042	−0.0043	0.0253	4.0159
2018	0.1057***	−0.0042	−0.0043	0.0253	4.3469
2019	0.1039***	−0.0042	−0.0043	0.0255	4.2453
2020	0.1249***	−0.0042	−0.0043	0.0256	5.0456

Notes: ***$p < 0.01$. Computations are based on 10,000 random permutations.

Conversely, the LL cluster portrays a contrasting picture, showcasing a decline in all types of metrics. In tandem, the LH cluster reflects a complex shift — an increase in CO_2 emissions in million tons and CO_2 emissions per unit of industrial GVA, juxtaposed with a decrease in per-capita CO_2 emissions. Lastly, the HL cluster presents a scenario of increased CO_2 emissions in million tons, counterbalanced by a decrease in both per-capita CO_2 emissions and CO_2 emissions per unit of industrial GVA. Geographically, the influence of the HH type predominantly emerged in the east, center, and southeast of the EU, while the LL type concentrated in the western and northern regions. A strong dependency on fossil-fueled energy production marks HH clusters. Those also count with a concentration of industry facilities from sectors that require technological innovation to decarbonize (e.g., cement, chemicals, ceramics). The development and adoption of technological innovation that allows emission reduction from carbon-intensive industrial activities is still ongoing, and the lack of necessary resources in the territory might delay this process. LL clusters present a low number of energy and industry facilities, but their superior performance should not be exclusively attributed to a territorial context that is less carbon-dependent. A higher presence of skilled labor and specialized knowledge, coupled with the diffusion of cleaner technologies and sustainable practices, is likely what facilitates this process.

3.5. Spatiotemporal transition

The findings presented in Table 3 illustrate a consistent pattern where all diagonal elements surpass their off-diagonal counterparts. This pattern signifies that, irrespective of the specific spatial hysteresis at play, a region tends to maintain its initial categorization over subsequent years more often than transitioning to other types. Notably, from 2008 to 2014, the transition from LH_t to LL_{t+1} exhibited the highest probability (0.114), resulting in 35 transferred units. Similarly, the transition from LH_t to LL_{t+1} held the highest probability (0.078) between 2014 and 2020, involving 25 transferred units. In aggregate, LH_t to LL_{t+1} demonstrated the highest overall transfer probability (0.096), encompassing 61 transferred county units throughout the entire period from 2008 to 2020. The predominance of a transition pattern towards lower emissions is a small positive signal that a European region's adoption of new low-carbon practices and technologies tends to be transferred to its neighbors. However, the observed dominance of a type IV classification (0.923) indicates no transitions in the unit or the neighborhood. This pattern suggests a notably higher degree of path dependence and lock-in characteristics in spatial agglomeration. Additionally, transition ratios for types I, II, and III were 0.026, 0.049, and 0.002, respectively. This indicates that the second strongest pattern observed in the time-space transition matrix is Type II, which underscores the dynamic nature of neighborhood-level changes and their influence on carbon emissions within the studied units.

4. Conclusions

This study explored the decarbonization landscape of EU energy and heavy-industry sectors at the regional level considering spatiotemporal interconnections. From a methodological perspective, the employment of ESTDA techniques is highly effective in examining the spatiotemporal coupling dynamics of carbon emissions. This approach provided a

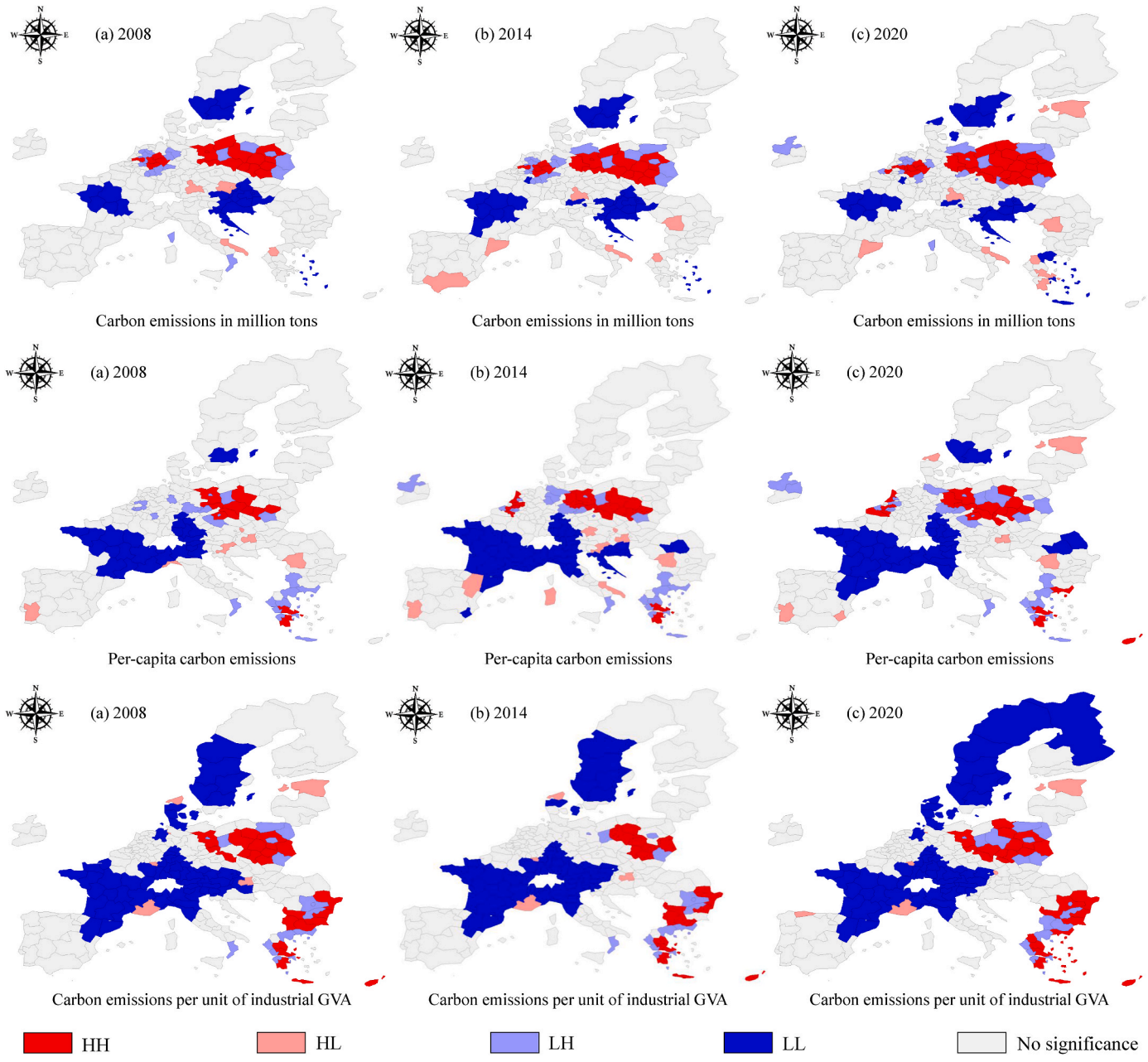

Fig. 7. Spatial agglomeration of regional carbon emissions in the EU.

Table 3
Space-time transition and probability matrix of regional CO_2 emissions at different stages.

Period of time	t/t+1	HH	LH	LL	HL	Type	n	Proportion	S_t
2008–2014	HH	0.938	0.031	0.004	0.027	I	38	0.027	0.921
	LH	0.006	0.877	0.114	0.003	II	72	0.050	
	LL	0.000	0.038	0.942	0.020	III	3	0.002	
	HL	0.024	0.004	0.064	0.908	IV	1315	0.921	
2014–2020	HH	0.948	0.019	0.005	0.028	I	37	0.026	0.926
	LH	0.038	0.884	0.078	0.000	II	67	0.047	
	LL	0.002	0.042	0.938	0.018	III	2	0.001	
	HL	0.034	0.000	0.038	0.928	IV	1322	0.926	
2008–2020	HH	0.943	0.025	0.005	0.028	I	75	0.026	0.923
	LH	0.022	0.881	0.096	0.002	II	139	0.049	
	LL	0.001	0.040	0.940	0.019	III	5	0.002	
	HL	0.029	0.002	0.051	0.918	IV	2637	0.923	

comprehensive understanding of the heterogeneity and regional characteristics inherent in European carbon emissions and underscored the trend of regional shifts influenced by the surrounding context in adjacent years.

Our findings demonstrate that European industrial carbon emissions are reducing and energy efficiency has increased, testifying that carbon-intensive industrial sectors are aligned with EU decarbonization policies. Although a general decline in emissions is present, the more significant results relate to efficiency improvements, as shown by relative indicators that compare emissions reductions with demographic and economic activity, such as a 34.8 % reduction in per-capita emissions and a 40.4 % reduction in emissions per industrial GVA unit. Those figures imply the efficacy of emission reduction initiatives in decoupling emissions from population growth and maintaining or elevating production levels with reduced emissions. Such success likely can be attributed to adopting technologies aimed at enhancing energy efficiency, expanding renewable energy sources, and fostering sustainable consumption practices. Consequently, this demonstrates that current policies for advancing energy efficiency and renewable energy adoption have achieved results; however, the question of whether this is sufficient looms large, particularly in the context of achieving a net-zero target in three decades.

Our findings also demonstrate an overall decreasing trend in regional disparities in carbon emissions. This downward trend may suggest a plateau in the mitigation potential of carbon reduction practices in energy and heavy-industry sectors. This potential plateau reinforces the limitations of actions aimed at optimizing current production processes to meet the targets set for 2050. Breakthrough innovations are required to accelerate the industrial transition, such as membrane technology in the (petro)-chemical industry, carbon-neutral steelmaking, alternative feedstock for cement production, and carbon capture and storage (Gerres et al., 2019).

Our analysis of regional emissions data with a spatial correlation approach suggests a pronounced spatial aggregation towards cluster polarization, with some clusters of regions successfully decarbonizing industrial activities while others are not achieving the desired results. Clusters of regions with higher emissions are observed to increase and concentrate in the central-east macro-region. Regions with a strong dependency on coal for energy generation, such as those in Greece and Poland, exhibit high emissions and cluster with neighboring regions similarly characterized by elevated emissions. In contrast, regions prioritizing renewables, exemplified by those in Sweden and Denmark, demonstrate lower and swiftly declining emissions. This outcome emphasizes the need for targeted interventions in regions with persistent carbon intensity to facilitate decarbonization.

Additionally, the analysis of space-time transitions suggests a tendency for regions to maintain their decarbonization pattern, with the highest probability indicating no transfer and the second-highest probability suggesting a shift from HL to LL clusters, representing the most frequent transfer occurrence. Regions that have transitioned from high to low emissions typically start from elevated emission levels and achieve emission reduction through mechanisms such as technology transfer, competition, or imitation effects (Wang et al., 2018).

Policy implications can be drawn from this study. Firstly, the results confirm the effectiveness of EU policies in driving the decarbonization process. These policies have been successful to the extent that much of what could be achieved quickly – namely, the "low-hanging fruits" of decarbonization – has already been realized. Secondly, the analysis at the regional level has shown how regions with similar decarbonization paths may belong to different Member States. Thus, policymakers are invited to consider categorizing European regions based on clusters, like the ones identified by this study, that relate to regions' decarbonization paths and advancing policy instruments targeted to those contexts. Different clusters of regions may present structural similarities between them (e.g., similar energy sources and industrial specialization). Developing targeted policies for these different clusters can be an effective avenue to help Europe advance its decarbonization goal instead of proposing similar interventions to all (Baudino, 2020; Liu et al., 2023; Lian et al., 2024; Shon et al., 2024). In particular, targeted policies to support regions that have not yet started their decarbonization journey are needed (e.g., regions in Greece and Poland). One example of policy intervention involves setting more ambitious decarbonization targets for clusters with stronger capacity to reduce emissions, accelerate their transition, and reinforce their leadership role. Another possible policy measure could be financial incentives that aim at the clusters' specific needs. Considering the LL cluster, investments in developing new radical low-carbon technologies, societal innovations, and different economic models may be required (i.e., post-growth theories, see Hardt and O'Neill, 2017). In contrast, for the HH cluster, investments in technologies already available might provide more rapid decarbonization results. Policy should also foster the sharing of best practices between regions with similar decarbonization pathways (LL and HH) and with different ones (LH and HL). Previous studies suggest that coordinated investments in tertiary education and research and development have been demonstrated to be effective drivers in the EU context (Vagnini et al., 2025). Regional governments can play a key role in mobilizing resources, fostering innovation, and facilitating the development of sustainable practices.

This study has some shortcomings and limitations that can be tackled in future studies. First, data analyzed in this study is up to the year 2020. This temporal boundary limits our ability to assess whether the spatial dynamics and regional disparities observed in the pre-pandemic period have persisted or evolved in recent years. However, based on provisional national-level data, it appears that the declining trend in industrial CO_2 emissions has continued beyond 2020 (EEA, 2024). Future studies could extend the temporal scope by incorporating data from the post-2020 period in order to capture potential long-term structural changes and validate the continuity of observed trends. Second, our analysis only considered emissions data from hard-to-abate industrial sectors. Broadening the scope to include data sources from other sectors that contribute to European carbon emissions could provide a more complete understanding of the barriers and prospects associated with achieving a net-zero emissions target. Third, our analysis focused on three variables: carbon emissions in million tons, per-capita carbon emissions, and carbon emissions per unit of industrial GVA. Future studies could include key drivers of carbon emissions, such as institutional factors (e.g., quality of regulations and standards), industrial-specific factors (e.g., energy mix use, the number of facilities, employment levels, technological innovation, and environmental practices), imports and potential exports beyond the EU (with particular focus on major contributors like China), and the role of both endogenous and imported technologies, which are crucial for supporting Europe's transition to cleaner industrial structures. Fourth, this study focused on the regional level. Future research could refine the unit of analysis by moving to a lower geographical scale, such as industrial hotspots, poles or hubs, or by focusing on the representative clusters identified in this study. This would allow a deeper characterization of the European decarbonization process and a more detailed analysis of which sectors are facing carbon lock-ins. Lastly, this study does not propose targeted and actionable measures to achieve net-zero industrial emissions within the required timeframe; rather, it highlights spatiotemporal evolution, polarized characteristics, and patterns of spatial aggregation of carbon emissions across EU regions. Future studies could build on these findings to explore specific decarbonization pathways, technological solutions, policy mechanisms, and the interaction between industrial transformation and spatial planning.

CRediT authorship contribution statement

Chiara Vagnini: Writing – original draft, Visualization, Methodology, Formal analysis, Data curation, Conceptualization. **Leticia Canal Vieira:** Writing – review & editing, Formal analysis, Conceptualization.

Mariolina Longo: Writing – review & editing, Supervision, Project administration, Conceptualization. **Matteo Mura:** Writing – review & editing, Supervision, Project administration, Conceptualization.

Declaration of competing interest

The authors declare that they have no known competing financial interests or personal relationships that could have appeared to influence the work reported in this paper.

Appendix A. Supplementary data

Supplementary data to this article can be found online at https://doi.org/10.1016/j.jenvman.2025.126466.

Data availability

Data will be made available on request.

References

Anselin, L., 1988. Spatial econometrics: Methods and models. Springer.

Anselin, L., 1995. Local indicators of spatial association-LISA. Geogr. Anal. 27, 93–115. https://doi.org/10.1111/j.1538-4632.1995.tb00338.x.

Anselin, L., 1996. The Moran scatterplot as an ESDA tool to assess local instability in spatial association. In: Fisher, M., Scholten, H.J., Unwin, D. (Eds.), Spatial Analytical Perspectives on GIS. Taylor & Francis, London.

Anselin, L., 2001. Spatial econometrics. In: Baltagi, B. (Ed.), Companion to Econometrics. Basil Blackwell, Oxford.

Anselin, L., Bao, S., 1997. Exploratory spatial data analysis linking SpaceStat and ArcView. In: Fisher, M., Getis, A. (Eds.), Recent Developments in Spatial Analysis. Springer, Berlin Heidelberg NewYork.

Anselin, L., Bera, A., 1998. Spatial dependence in linear regression models with an introduction to spatial econometrics. In: Ullah, A., Giles, D. (Eds.), Handbook of Applied Economic Statistics. Marcel Dekker, New York, pp. 237–289.

Barbero, J., Mandras, G., Rodríguez-Crespo, E., Rodríguez-Pose, A., 2021. Quality of government and regional trade: evidence from European Union regions. Reg. Stud. 55 (7), 1240–1251. https://doi.org/10.1080/00343404.2021.1873934.

Bataille, C., Nilsson, L.J., Jotzo, F., 2021. Industry in a net-zero emissions world: new mitigation pathways, new supply chains, modelling needs and policy implications. Energy Clim. Change 2, 100059. https://doi.org/10.1016/j.egycc.2021.100059.

Baudino, M., 2020. Environmental Engel curves in Italy: a spatial econometric investigation. Pap. Reg. Sci. 99 (4), 999–1019. https://doi.org/10.1111/pirs.12521.

Boschma, R.A., Frenken, K., 2006. Why is economic geography not an evolutionary science? Towards an evolutionary economic geography. J. Econ. Geogr. 6 (3), 273–302. https://doi.org/10.1093/jeg/lbi022.

Cliff, A.D., Ord, J.K., 1981. Spatial Processes: Models and Applications. Pion, London.

Crippa, M., Guizzardi, D., Banja, M., Solazzo, E., Muntean, M., Schaaf, E., Pagani, F., Monforti-Ferrario, F., Olivier, J., Quadrelli, R., et al., 2022. CO_2 Emissions of all World Countries - 2022 Report, EUR 31182 EN. Publications Office of the European Union, Luxembourg. https://doi.org/10.2760/730164.

Diakoulaki, D., Mandaraka, M., 2007. Decomposition analysis for assessing the progress in decoupling industrial growth from CO2 emissions in the EU manufacturing sector. Energy Econ. 29 (4), 636–664. https://doi.org/10.1016/j.eneco.2007.01.005.

European Environment Agency (EEA), 2024. Progress towards national greenhouse gas emissions targets in Europe. https://www.eea.europa.eu/en/analysis/indicators/progress-towards-national-greenhouse-gas?activeAccordion=546a7c35-9188-4d23-94ee-005d97c26f2b. (Accessed 20 May 2025).

European Commission, 2019. A European green deal. https://ec.europa.eu/info/strategy/priorities-2019-2024/europeangreen-deal_en. (Accessed 22 May 2024).

EUROSTAT. Regions in the European Union: nomenclature of territorial units for statistics NUTS 2013/EU-28. *Statistics*. https://doi.org/10.2785/15544.

Fazio, G., Maioli, S., Rujimora, N., 2024. Building back greener, levelling-up or both? An assessment of the economic and environmental efficiency transition of UK regions. Pap. Reg. Sci. 103 (6), 100053. https://doi.org/10.1016/j.pirs.2024.100053.

Gerres, T., Ávila, J.P.C., Llamas, P.L., San Román, T.G., 2019. A review of cross-sector decarbonisation potentials in the European energy intensive industry. J. Clean. Prod. 210, 585–601. https://doi.org/10.1016/j.jclepro.2018.11.036.

Grodzicki, T., Jankiewicz, M., 2022. The impact of renewable energy and urbanization on CO2 emissions in Europe–Spatio-temporal approach. Environ. Dev. 44, 100755. https://doi.org/10.1016/j.envdev.2022.100755.

Hardt, L., O'Neill, D.W., 2017. Ecological macroeconomic models: assessing current developments. Ecol. Econ. 134, 198–211. https://doi.org/10.1016/j.ecolecon.2016.12.027.

IPCC, 2018. Special report: global warming of 1.5 °C. https://www.ipcc.ch/sr15/chapter/spm/.

IPCC, 2023. Summary for Policymakers. In: Core Writing Team, Lee, H., Romero, J. (Eds.), Climate Change 2023: Synthesis Report. Contribution of Working Groups I, II and III to the Sixth Assessment Report of the Intergovernmental Panel on Climate Change. IPCC, Geneva, Switzerland, pp. 1–34 doi: 10.59327/IPCC/AR6-9789291691647.001.

Le Quéré, C., Andrew, R.M., Friedlingstein, P., Sitch, S., Hauck, J., Pongratz, J., et al., 2018. Global carbon budget 2018. Earth Syst. Sci. Data 10 (4), 2141–2194. https://doi.org/10.5194/essd-10-2141-2018.

Lian, Y., Lin, X., Luo, H., Zhang, J., Sun, X., 2024. Distribution characteristics and influencing factors of household consumption carbon emissions in China from a spatial perspective. J. Environ. Manag. 351, 119564. https://doi.org/10.1016/j.jenvman.2023.119564.

Liu, X., Jin, X., Luo, X., Zhou, Y., 2023. Quantifying the spatiotemporal dynamics and impact factors of China's county-level carbon emissions using ESTDA and spatial econometric models. J. Clean. Prod. 410, 137203. https://doi.org/10.1016/j.jclepro.2023.137203.

Liu, X., Zhang, L., Hao, Y., Yin, X., Shi, Z., 2022. Increasing disparities in the embedded carbon emissions of provincial urban households in China. J. Environ. Manag. 302, 113974. https://doi.org/10.1016/j.jenvman.2021.113974.

Moran, P.A., 1948. The interpretation of statistical maps. J. Roy. Stat. Soc. B 10, 243–251. https://doi.org/10.1111/j.2517-6161.1948.tb00012.x.

Mura, M., Longo, M., Toschi, L., Zanni, S., Visani, F., Bianconcini, S., 2021. The role of geographical scales in sustainability transitions: an empirical investigation of the European industrial context. Ecol. Econ. 183, 106968. https://doi.org/10.1016/j.ecolecon.2021.106968.

Mura, M., Longo, M., Zanni, S., Toschi, L., 2023. Exploring socio-economic externalities of development scenarios. An analysis of EU regions from 2008 to 2016. J. Environ. Manag. 332, 117327. https://doi.org/10.1016/j.jenvman.2023.117327.

Peiró-Palomino, J., Picazo-Tadeo, A.J., Rios, V., 2020. Well-being in European regions: does government quality matter? Pap. Reg. Sci. 99 (3), 555–582. https://doi.org/10.1111/pirs.12494.

Rey, S., 2014. Rank-based Markov chains for regional income distribution dynamics. J. Geogr. Syst. 16, 115–137. https://doi.org/10.1007/s10109-013-0189-0.

Rios, V., 2017. What drives unemployment disparities in European regions? A dynamic spatial panel approach. Reg. Stud. 51 (11), 1599–1611. https://doi.org/10.1080/00343404.2016.1216094.

Rios, V., Gianmoena, L., 2018. Convergence in CO_2 emissions: a spatial economic analysis with cross-country interactions. Energy Econ. 75, 222–238. https://doi.org/10.1016/j.eneco.2018.08.009.

Rissman, J., Bataille, C., Masanet, E., Aden, N., Morrow III, W.R., Zhou, N., et al., 2020. Technologies and policies to decarbonize global industry: review and assessment of mitigation drivers through 2070. Appl. Energy 266, 114848.

Rosenblatt, M., 1956. Remarks on some nonparametric estimates of a density function. Ann. Math. Stat. 832–837. https://doi.org/10.1214/aoms/1177728190.

Santoalha, A., Consoli, D., Castellacci, F., 2021. Digital skills, relatedness and green diversification: a study of European regions. Res. Pol. 50 (9), 104340. https://doi.org/10.1016/j.respol.2021.104340.

Shon, H., Lee, H., Kim, B., 2024. Spatial pattern of aid allocation in the early 21st century: Evidence from 38 sub-Saharan African countries. Papers in Regional Science 103 (3), 100026. https://doi.org/10.1016/j.pirs.2024.100026.

Sporkmann, J., Liu, Y., Spinler, S., 2023. Carbon emissions from European land transportation: a comprehensive analysis. Transport. Res. D: Transp. Environ. 121, 103851. https://doi.org/10.1016/j.trd.2023.103851.

Stuhlmacher, M., Patnaik, S., Streletskiy, D., Taylor, K., 2019. Cap-and-trade and emissions clustering: a spatial-temporal analysis of the European Union emissions trading scheme. J. Environ. Manag. 249, 109352. https://doi.org/10.1016/j.jenvman.2019.109352.

Sun, T., Ocko, I.B., Sturcken, E., Hamburg, S.P., 2021. Path to net zero is critical to climate outcome. Sci. Rep. 11 (1), 22173.

Theil, H., 1967. Economics and Information Theory. North-Holland Pub, Amsterdam.

Vagnini, C., Canal Vieira, L., Longo, M., Mura, M., 2025. Regional drivers of industrial decarbonisation: a spatial econometric analysis of 238 EU regions between 2008 and 2020. Reg. Stud. 59 (1), 2380369. https://doi.org/10.1080/00343404.2024.2380369.

Vieira, L., Longo, M., Mura, M., 2022. Will the regime ever break? Assessing socio-political and economic pressures to climate action and European oil majors' response (2005-2019). Clim. Policy 22 (4), 488–501. https://doi.org/10.1080/14693062.2022.2044283.

Wang, J., Hu, M., Rodrigues, J.F.D., 2018. An empirical spatiotemporal decomposition analysis of carbon intensity in China's industrial sector. J. Clean. Prod. 195, 133–144. https://doi.org/10.1016/j.jclepro.2018.05.185.

Xiao, H., Shan, Y., Zhang, N., Zhou, Y., Wang, D., Duan, Z., 2019. Comparisons of CO2 emission performance between secondary and service industries in Yangtze River Delta cities. J. Environ. Manag. 252, 109667. https://doi.org/10.1016/j.jenvman.2019.109667.

Xiaomin, G., Chuanglin, F., 2023. How does urbanization affect energy carbon emissions under the background of carbon neutrality? J. Environ. Manag. 327, 116878. https://doi.org/10.1016/j.jenvman.2022.116878.

Yang, S., Duan, Z., Jiang, X., 2023. Spatial dynamics and influencing factors of carbon rebound effect in tourism transport: evidence from the Yangtze-river delta urban agglomeration. J. Environ. Manag. 344, 118431. https://doi.org/10.1016/j.jenvman.2023.118431.

You, W., Lv, Z., 2018. Spillover effects of economic globalization on CO_2 emissions: a spatial panel approach. Energy Econ. 73, 248–257. https://doi.org/10.1016/j.eneco.2018.05.016.

Zhang, H., Li, S., 2022. Carbon emissions' spatial-temporal heterogeneity and identification from rural energy consumption in China. J. Environ. Manag. 304, 114286. https://doi.org/10.1016/j.jenvman.2021.114286.

Zhang, Z., Shi, K., Tang, L., Su, K., Zhu, Z., Yang, Q., 2022. Exploring the spatiotemporal evolution and coordination of agricultural green efficiency and food security in China using ESTDA and CCD models. J. Clean. Prod. 374, 133967. https://doi.org/10.1016/j.jclepro.2022.133967.